

# Magnetic Tunnel Junctions

## Introduction

Magnetic tunnel junctions or MTJs are nanostructured devices within the field of magnetoelectronics or spin electronics, hereafter called spintronics. In this area, the experimental observation of sizable and tunable magnetoresistance (change of materials resistance due to external magnetic fields) is intimately related to the exploitation of not only charge of the electron but also its spin. The discovery of giant magnetoresistance (GMR; [Barthélémy \*et al.\* 1999](#); see *Giant Magnetoresistance*) in multilayered ferromagnetic films separated by thin metallic spacers has initiated an enormous research interest, particularly also for a wealth of potential applications, e.g., in data-storage devices. Fueled by these developments and earlier efforts in tunneling devices ([Tedrow and Meservey 1971](#), [Jullière 1975](#)), [Moodera \*et al.\* \(1995\)](#) and [Miyazaki and Tezuka \(1995\)](#) have discovered that the tunneling current between two ferromagnetic films separated by a thin oxide layer strongly depends on an external magnetic field, an effect now known as tunnel magnetoresistance (TMR). Since then, the impact of MTJs on the field of spintronics has hugely expanded, particularly due to the enormous magnitude of the observed magnetoresistances at room temperature and its impact on potential applications ([Chappert \*et al.\* 2007](#)). The aim of this article is to first introduce the basic phenomenon of tunnel magnetoresistance in MTJs (Sect. 1). Subsequently, in Sect. 2, the key physical concepts for spin tunneling will be sketched by addressing a number of vital contributions—mostly using  $\text{Al}_2\text{O}_3$  as a barrier material—for understanding the physics behind TMR. Experiments using crystalline  $\text{MgO}$  barriers have dramatically improved the magnitude of TMR (see Sect. 3), and show that in clean systems the electronic structure of the complete tunneling junction may lead to enormous spin-selectivity. Section 4 is the conclusion of this article.

### 1. Basic Phenomena in MTJs

When electrons are tunneling between two ferromagnetic metals, the magnitude of the tunneling current depends on the relative orientation of the magnetization of both electrodes (see [Fig. 1](#)). This can be understood from a few elementary arguments: (i) the tunneling current is, in first order, proportional to the product of the electrode density of states (DOS) at the Fermi level; (ii) in ferromagnetic materials, the ground-state energy bands in the vicinity of the Fermi level are shifted in energy, yielding separate majority and minority bands for

electrons with opposite spins; and (iii) assuming spin conservation for the tunneling electrons, there are two parallel currents of spin-up and spin-down character. As a result of these aspects, the current between electrodes with the same magnetization direction should be higher than those with opposite magnetization (see [Fig. 1](#)).

Within this simple model, the change in resistance between antiparallel and parallel magnetization (normalized to the parallel resistance) is given by

$$\text{TMR} = \frac{2P_1P_2}{1 - P_1P_2} \quad \text{with } P_{1,2} = \frac{N_{1,2}^{\text{maj}} - N_{1,2}^{\text{min}}}{N_{1,2}^{\text{maj}} + N_{1,2}^{\text{min}}} \quad (1)$$

where  $P_{1,2}$  are the so-called tunneling spin polarizations determined by the relative difference in DOS at the Fermi level. It is crucial to realize that not all electrons present at the Fermi level can efficiently tunnel through the barrier, and that this simple equation is not able to capture the physics behind a number of observations in MTJs. As discussed in Sect. 2, in many cases the spherically symmetric  $s$ -like electrons, which have a much lower DOS at the Fermi level, dominantly tunnel through the barrier, and the interface between the insulating tunnel barrier and the ferromagnets plays an essential role. Nonetheless, this expression clearly demonstrates the presence of a magnetoresistance effect and

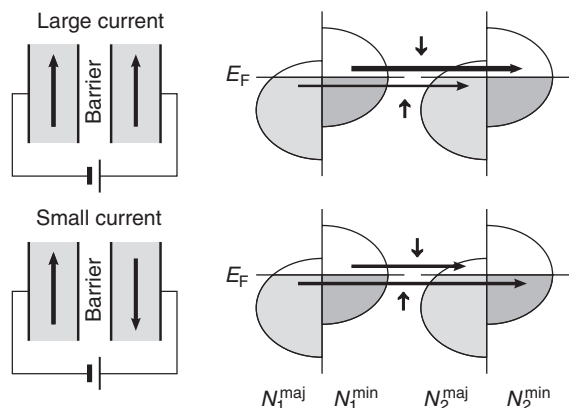


**Figure 1**

Schematic illustration showing the mechanism of TMR. Top: for parallel aligned magnetization as sketched at left, electrons around the Fermi level with spin up ( $\uparrow$ ) and spin down ( $\downarrow$ ) are allowed to tunnel from majority to majority bands, and from minority to minority bands. Bottom: when the magnetization is antiparallel, tunneling takes place from majority to minority and minority to majority bands, leading to a reduction of total tunneling current. In terms of electrical resistance, this corresponds to a higher resistance when the magnetization of the two layers is oppositely aligned.

the relevance of the magnetic character for the spin polarization of the tunneling electrons. Moreover, it shows that so-called half-metallic metals (see *Half-metallic Magnetism*) with only one of the two spin species available at the Fermi level (De Groot *et al.* 1983) may, in principle, engender infinitely high TMR. Indications for such behavior are indeed observed, for instance, in  $\text{La}_{2/3}\text{Sr}_{1/3}\text{MnO}_3/\text{SrTiO}_3/\text{La}_{2/3}\text{Sr}_{1/3}\text{MnO}_3$  (Bowen *et al.* 2003) and  $\text{Co}_2\text{FeAl}_{0.5}\text{Si}_{0.5}/\text{Al}_2\text{O}_3/\text{Co}_2\text{FeAl}_{0.5}\text{Si}_{0.5}$  (Tezuka *et al.* 2007).

An important aspect for the presence of TMR is the ability to independently manipulate the direction of the magnetization of the electrodes. This can be accomplished by several methods which include the (sometimes combined) use of intrinsic differences in magnetic hysteresis of the ferromagnetic materials, exchange biasing with antiferromagnetic thin films (Coehoorn 2003), and antiferromagnetic interlayer coupling across nonmagnetic metallic films (see *Multilayers: Interlayer Coupling*). Figure 2 shows the room-temperature resistance change for a MJT with a MgO barrier. Two soft-magnetic CoFeB electrodes with different coercivities are used to create a clear distinction between the resistance levels in parallel and antiparallel alignment of the magnetization.

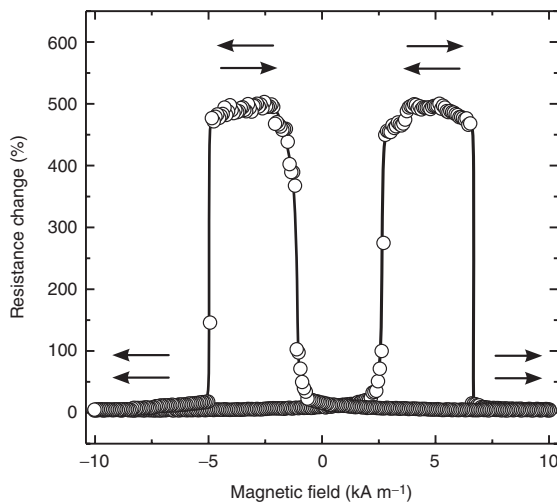


**Figure 2**

Resistance change in a magnetic tunnel junction consisting of  $(\text{Co}_{25}\text{Fe}_{75})_{80}\text{B}_{20}/2.1\text{ nm MgO}/(\text{Co}_{25}\text{Fe}_{75})_{80}\text{B}_{20}$ . The data are taken at room temperature. The arrows indicate the orientation of the CoFeB magnetization. Adapted from Lee Y M, Hayakawa J, Ikeda S, Matsukura F, Ohno H 2007 Effect of electrode composition on the tunnel magnetoresistance of pseudo-spin-valve magnetic tunnel junction with a MgO tunnel barrier. *Appl. Phys. Lett.* **90** (3), 212507.

## 2. Key Ingredients for TMR

This section discusses some of the developments which shed new light on the physics of MTJs. It should be realized that the focus of this article is on a limited selection out of a great number of excellent and relevant contributions. More extended review papers are available (see, e.g., Swagten 2007), and, among other issues, address the important role of the temperature dependence of TMR and the applied bias voltage between the electrodes. In order to guide the reader through the contributions highlighted here, Fig. 3 shows a number of engineered tunneling structures that are discussed later in this article.

Tedrow and Meservey (1971) report the first experiments on spin tunneling. In their case, only one electrode is ferromagnetic (Ni), the other being a superconductor (Al). They have found that though minority electrons dominate the DOS at the Fermi level of Ni, majority electrons are most efficiently tunneling through the thin  $\text{Al}_2\text{O}_3$  barrier ( $P > 0$ ). Later, it is suggested by Hertz and Aoi (1973) and Stearns (1977) that, although the dominant species of electrons at the Fermi level of transition metal ferromagnets are minority  $d$ -electrons, they do not couple well with the states over the barrier. Instead, highly dispersive majority  $s$ -like electrons have a much larger overlap integral with states in the barrier which leads to a larger transmission probability for these electrons. Moreover, the interaction between the  $s$ - and  $d$ -electrons ( $s$ - $d$  hybridization) leads to a suppression of the  $s$ -DOS in regions of large  $d$ -DOS, which is also the case at the Fermi level of a  $3d$  transition metal ferromagnet. Consequently, this induces a spin polarization of the  $s$ -DOS at the Fermi energy.

After these seminal papers on ferromagnetic tunneling, including the first prediction of a TMR effect by Jullière (1975), it took around two decades to do the same experiment with two ferromagnetic electrodes, as mentioned in the introduction (Moodera *et al.* 1995, Miyazaki and Tezuka 1995). It should be noted that in all these experiments  $\text{Al}_2\text{O}_3$  is preferred as barrier material, primarily since it allows an easy growth of a pinhole-free thin barrier by natural, thermal, or plasma oxidation of Al thin films. Figure 3(a) shows the layout of such an MTJ. Experimentally, a positive TMR is almost exclusively observed since usually two transition metal ferromagnets are combined that have a spin polarization  $P$  with the same (positive) sign (see Eqn. 1). On the theoretical side, there has been considerable effort to model tunneling through  $\text{Al}_2\text{O}_3$  (see, e.g., Slonczewski 1989, Tsymbal and Pettifor 1997, Oleinik *et al.* 2000). However, due to its amorphous structure which hinders *ab initio* calculations, despite persistent effort, our theoretical understanding of tunneling through  $\text{Al}_2\text{O}_3$  has remained limited. Therefore, many experimental

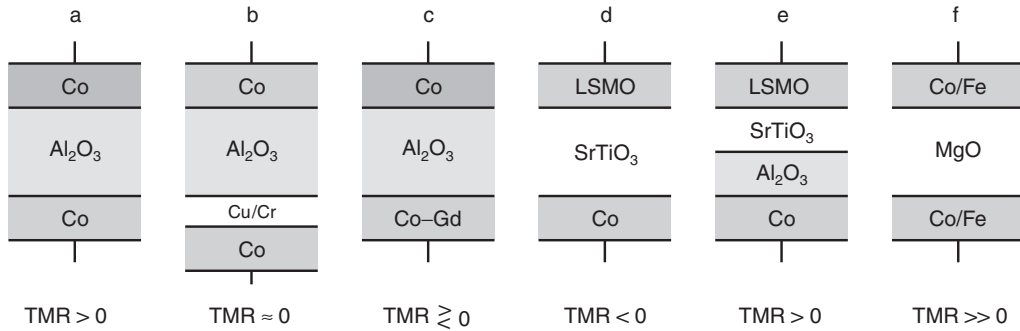


**Figure 3**

(a–f) A number of basic configurations showing, for example, the role of the barrier/electrode combination in relation to the sign and magnitude of the TMR effect; these cartoons are used throughout this paper; see the text.

attempts were made to address these issues, which are discussed here. Nevertheless, theory has provided vital evidences that the interface between the barrier and the ferromagnet, and the relevant chemistry or bonding at such an interface, is crucial for spin tunneling. For example, using first-principles calculations, [Belashchenko et al. \(2005\)](#) predicted a sign change for the spin polarization of tunneling electrons depending on where oxygen atoms sit on a Co surface.

Earlier, we have discussed that TMR is directly related to the tunneling spin polarization ( $P$ ) induced by the ferromagnetic DOS. One may imagine that  $P$  is not constant over the whole Fermi surface, and varies depending on which direction in  $k$ -space one probes, that is, on the crystallographic orientation of the electrode at the interface with the tunnel barrier. The demonstration of such crystal anisotropy of the TMR is given by [Yuasa et al. \(2000\)](#), who have shown that the use of single-crystalline Fe electrodes of different orientations in MTJs resulted in a substantially different TMR.

Inserting an additional layer at the barrier–ferromagnet interface (see [Fig. 3\(b\)](#)) has been investigated to rigorously probe the origin of tunneling spin polarization  $P$ . [LeClair et al. \(2000\)](#) show that inserting one monolayer of Cu between the bottom Co electrode and the Al<sub>2</sub>O<sub>3</sub> barrier leads to a strong reduction of TMR. Their results are shown in [Fig. 4\(a\)](#). Moreover, while the TMR exponentially decays with a length scale of 2.6 Å for a Cu layer, a similar layer of antiferromagnetic Cr induces an even faster exponential decay on a length scale of 1.2 Å ([LeClair et al. 2001](#)). Not only do these results clearly demonstrate the limited applicability of Eqn. 1, but also the truly interfacial nature of the tunneling spin polarization  $P$ , illustrating that only a few monolayers adjacent to the tunnel barrier are important for tunneling.

[Yuasa et al. \(2002\)](#) have further developed these experiments by achieving sharp interfaces between single crystalline Co(001) and Cu(001) using

molecular beam epitaxy. Their MTJ stack and the corresponding TMR are shown in [Fig. 4\(b\)](#). They explain that majority electrons tunneling from NiFe into Co would transmit easily as compared to minority electrons which have a higher probability to be reflected at the Co–Cu interface (similar to the underlying reason for interlayer coupling; see *Multilayers: Interlayer Coupling*). If multiple scattering occurs between the Co–Cu and Cu–Al<sub>2</sub>O<sub>3</sub> interfaces, the minority electrons would form resonant quantum well states in the Cu layer, resulting in the oscillatory behavior of TMR. From the period of the oscillation, they derive that the quantum well states are formed in the  $\Delta_1$  band of Cu. The importance of the dominant contribution of this highly dispersive  $s$ -like  $\Delta_1$  band in tunneling through Al<sub>2</sub>O<sub>3</sub> is reiterated by [Nagahama et al. \(2005\)](#) who have fabricated single-crystalline MTJs with Cr(001) inserted at the interface, similar to the work of [LeClair et al. \(2001\)](#) (see [Fig. 3\(b\)](#)). They argue that, since the band structure of an epitaxial Cr layer has no band of  $\Delta_1$  symmetry at the Fermi level in the  $k_{\parallel} = 0$  direction, the electrons from one electrode can tunnel only if they are scattered at the interface of the other electrode due to the presence of the Cr layer. These results clearly show the importance of the spherically symmetric  $s$ -like electrons in tunneling through Al<sub>2</sub>O<sub>3</sub>.

Although most ferromagnets display a positive  $P$  in conjunction with Al<sub>2</sub>O<sub>3</sub>, [Kaiser et al. \(2005a\)](#) have reported that Co–Gd alloys can exhibit both positive and negative  $P$  systematically depending on the alloy composition. It is known that in these alloys the Co and Gd ferromagnetic subnetwork magnetization is aligned antiparallel with respect to each other, which may significantly influence the tunneling spin polarization. Now the sign of  $P$  depends on the orientation of the respective subnetwork magnetization with respect to the applied field. The  $P$  from either of these subnetworks will be positive when its magnetization is aligned with the applied magnetic field, in contrast

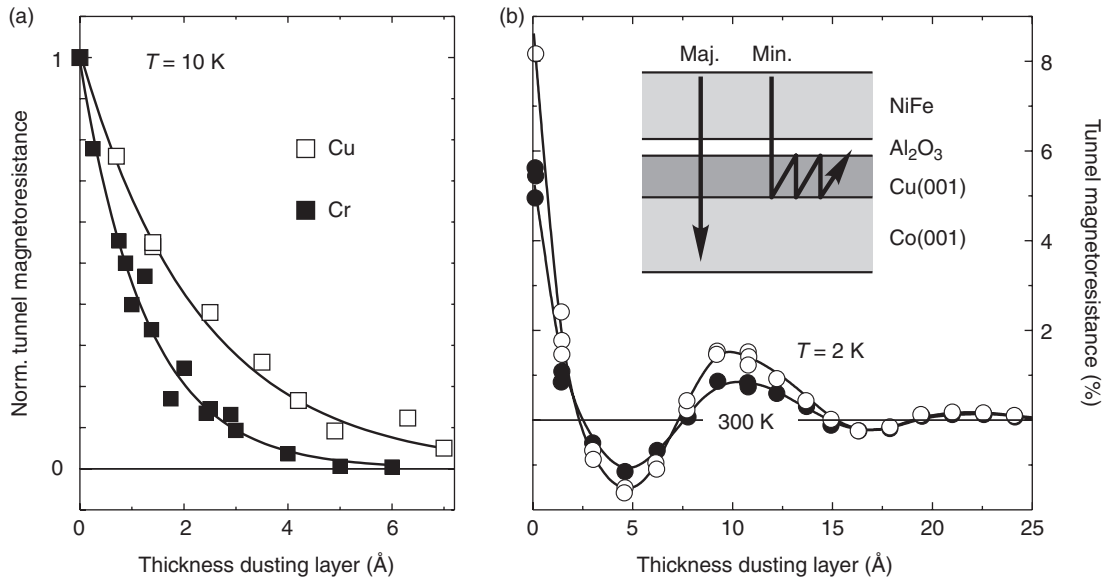


**Figure 4**

TMR when incorporating thin dusting layers at the barrier of an MTJ. (a) Normalized TMR data at  $T = 10$  K for sputtered  $\text{Co}/X/\text{Al}_2\text{O}_3/\text{Co}$  junctions, with  $X = \text{Cu}$  and  $\text{Cr}$  (LeClair *et al.* 2000, 2001). (b) TMR at  $T = 2$  K and 300 K as a function of the thickness of the Cu interface layer thickness in epitaxial  $\text{Co}(001)/\text{Cu}(001)/\text{Al}_2\text{O}_3/\text{NiFe}$ . The inset schematically shows quantum well reflections for minority electrons in the Cu layer when propagating perpendicular to the barrier ( $k_{\parallel} = 0$ ). Adapted from Yuasa S, Nagahama T, Suzuki Y 2002 Spin-polarized resonant tunneling in magnetic tunnel junctions. *Science* **297**, 234–7.

to the moments of the other subnetwork. Kaiser *et al.* (2005a) found that the measured  $P$  is the sum of independent spin-polarized tunneling currents from the Co and Gd subnetworks, resulting in a sign change of  $P$  with alloy composition. When combined with traditional ferromagnetic materials with positive  $P$  in an MTJ, this leads to positive or negative TMR, depending on the sign of the Co–Gd polarization (see Fig. 3(c)).

As we mentioned earlier, chemical bonding at the interface has been predicted to have a great influence on  $P$ . Such bonding would influence the tunneling matrix element occurring in Fermi's golden rule which couples initial and final state wave functions, depending on symmetry and overlap arguments. Consider the case of Co–Pt alloys studied by Kaiser *et al.* (2005b). They observe that the measured  $P$  does not change after alloying ferromagnetic Co with up to 40 at.% of nonmagnetic Pt, while the magnetic moment of the alloy reduces by  $\approx 40\%$  of its initial value for Co. They argue that the magnetic moment of Co in Co–Pt alloys, which does not change much from its value for pure Co, and the higher tunneling rate from Co atoms at the interface as compared to Pt atoms, are responsible for the almost constant  $P$  of Co–Pt alloys. The higher tunneling rate arises from the higher affinity of Co to bond with oxygen at the interface between Co–Pt and  $\text{Al}_2\text{O}_3$ . Kaiser *et al.* (2005b) estimate that

the tunneling probability from the Pt sites at the interface is  $\approx 3.8$  times lower than from the Co sites. This study suggests that it is possible to form MTJs with high  $P$  and TMR with low-magnetic-moment alloys by utilizing interface bonding effects and manipulating the tunneling rates of the alloy constituents.

Arguably, the most decisive experiments demonstrating the relevance of interface bonding effects are those of Sharma *et al.* (1999) and De Teresa *et al.* (1999). In the latter case, MTJs with  $\text{Co}/I/\text{La}_{2/3}\text{Sr}_{1/3}\text{MnO}_3$  (LSMO) were studied, where  $I$  could be  $\text{SrTiO}_3$  (STO),  $\text{Ce}_{0.69}\text{La}_{0.31}\text{O}_{1.845}$  (CLO), or  $\text{Al}_2\text{O}_3$ . In these experiments, the effective polarization of Co is found to be positive (majority electrons tunnel preferentially) with  $\text{Al}_2\text{O}_3$  as barrier, and negative (minority electrons tunnel preferentially) with STO or CLO as barrier. As the  $P$  of the STO–LSMO interface is known to be positive, the inverse TMR observed in Co/STO/LSMO junctions is the signature of a negative polarization of the Co–STO interface (see Fig. 3(d)). This inversion of the sign of  $P$  for the Co–STO interface with respect to the  $P$  of Co– $\text{Al}_2\text{O}_3$  is confirmed by growing  $\text{Co}/\text{Al}_2\text{O}_3/\text{STO}/\text{LSMO}$  junctions which also reveal a positive  $P$  for the Co– $\text{Al}_2\text{O}_3$  interface (Fig. 3(e)). The negative  $P$  of Co when the barrier is STO or CLO can be viewed as a preferential selection of electrons of  $d$ -character at the Co–STO and Co–CLO interfaces, as compared to the positive

$P$  in Co–Al<sub>2</sub>O<sub>3</sub> where the selection of electrons with  $s$ -character occurs at the interface. This negative  $P$  of the Co–STO interface has later been verified from first principles by [Velev \*et al.\* \(2005\)](#). These results again show that tunneling spin polarization (and therefore TMR) should be viewed as a property predominantly determined by the barrier–ferromagnet interface and strongly influenced by the chemistry at the interface.

### 3. Coherent Spin Tunneling and Giant TMR

As mentioned earlier, due to the amorphous nature of Al<sub>2</sub>O<sub>3</sub>, *ab initio* studies aiming at fundamental understanding of spin-dependent transport in tunnel junctions have been difficult to perform. Therefore, there has been a continuous effort to develop crystalline barriers which allow for coherent electron transport. The use of MgO barriers (and the observation of giant TMR) is discussed later specifically due to the paramount role it plays in our understanding of spin tunneling and due to its great impact for technological applications.

One aspect which is highly unlikely in tunneling through an amorphous barrier is  $k_{\parallel}$  conservation of the electron wave vector. On the contrary, in a crystalline barrier,  $k_{\parallel}$  conservation (also known as coherent tunneling) is a distinct possibility. This also

implies that a wave vector selected at one interface efficiently couples to a corresponding wave vector at the other interface. Keeping in mind that  $P$  is not constant over the whole Fermi surface, one could imagine that using a certain electrode–barrier interface in a certain crystallographic orientation would result in efficient electron tunneling for wave functions which have specific symmetries. This in turn could lead to a very large tunneling spin polarization, even though the averaged DOS at the Fermi level of the ferromagnet is only moderately polarized.

Among other systems, such a pseudo-half-metallic behavior has been theoretically predicted ([Butler \*et al.\* 2001](#), [Mathon and Umerski 2001](#)) for epitaxial Fe(001)/MgO(001)/Fe(001), and later also for other body-centered cubic (b.c.c.) ferromagnetic metals based on Fe and Co. In these tunnel junctions, there are three kinds of evanescent tunneling states in the bandgap of MgO (see [Fig. 5](#):  $\Delta_1$ ,  $\Delta_5$ ,  $\Delta_2'$ ) when coherently tunneling between the oriented Fe electrodes in the direction corresponding to  $k_{\parallel}=0$ . In parallel alignment of the Fe layers ([Fig. 5\(a\)](#)), it is shown that the  $\Delta_1$  states have only a very modest decay in MgO(001) as compared to the other states. In contrast, in antiparallel alignment the majority  $\Delta_1$  states that efficiently tunnel through the barrier cannot couple to the DOS of the other electrode due to the intrinsic absence of such a  $\Delta_1$  minority band at the Fermi level. This dominant role of the Fe

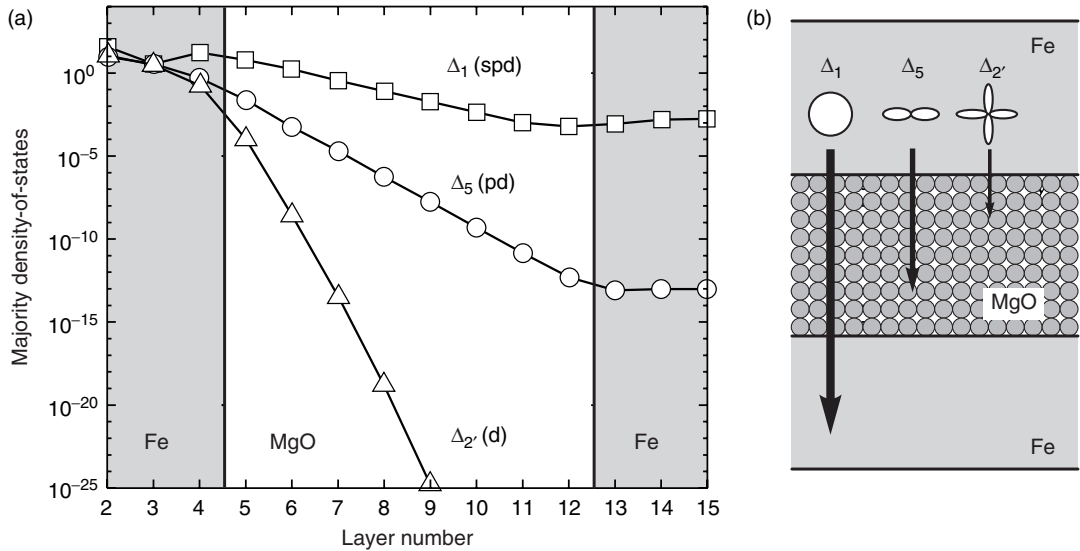


**Figure 5**

(a) Layer-resolved tunneling density-of-states for  $k_{\parallel}=0$  in Fe(001)/8 monolayers MgO/Fe(001) for majority electrons when the magnetization of the Fe layers is parallel oriented. Each curve is labeled by the symmetry of the incident Bloch state in the left Fe electrode, showing, for example, the slow decay of states with  $\Delta_1$  symmetry (in the  $\Gamma$ – $X$  direction in  $k$  space). Part (b) shows the strong differences in decay of these states. Adapted from [Butler W H, Zhang X G, Schulthess T C, MacLaren J M 2001 Spin-dependent tunneling conductance of Fe|MgO|Fe sandwiches. \*Phys. Rev. B\* 63 \(12\), 054416.](#)

$\Delta_1$ -MgO  $\Delta_1$ -Fe  $\Delta_1$  channel when coherently tunneling for  $k_{\parallel}=0$  leads to a very high spin polarization of the current, and hence a high (giant) TMR (see Fig. 3(f)).

After a number of initial efforts to observe this enormous spin selectivity in epitaxial junctions, the breakthrough in this field has been reported for epitaxial (001)-oriented Fe/MgO/Fe junctions (Yuasa *et al.* 2004) and sputtered CoFe/MgO/CoFe (Parkin *et al.* 2004), showing TMR ratios well above 100%, thereby substantially exceeding the magnetoresistance of Al<sub>2</sub>O<sub>3</sub>-based devices. Since then, the TMR of junctions involving MgO as a barrier has steadily been improved, in particular by using the ternary CoFeB alloy as the ferromagnetic electrode (Parkin *et al.* 2004, Djayaprawira *et al.* 2005). It is believed that high-quality MgO can be adequately stabilized between the as-grown, amorphous CoFeB electrodes, which, after annealing at temperatures up to almost 400°C, attain their required b.c.c. character. An example TMR of  $\approx 500\%$  at room temperature is shown in Fig. 2 for annealed (Co<sub>25</sub>Fe<sub>75</sub>)<sub>80</sub>B<sub>20</sub>/MgO/(Co<sub>25</sub>Fe<sub>75</sub>)<sub>80</sub>B<sub>20</sub> junctions. Due to these enormous magnetoresistances, there is an ongoing effort not only in explaining the large tunneling spin polarization of CoFeB (see, e.g., Paluskar *et al.* 2008), but also in further implementing CoFeB for novel spintronics devices and industrial applications (Chappert *et al.* 2007).

#### 4. Conclusion

In the field of spintronics, MTJs display magnetoresistance effects due to the spin dependence of the tunneling current when dealing with ferromagnetic electrodes. The physics behind TMR has been experimentally and theoretically explored by introducing novel concepts and engineered material combinations. This has dramatically increased our knowledge of tunneling between ferromagnetic materials.

See also: Giant Magnetoresistance; Half-metallic Magnetism; Magnetic Recording Systems: Spin Electronics; Magnetic Recording Systems: Spin Valves; Magnetoresistive Heads: Physical Phenomena; Magnetic Tunnel Transistor; Multilayers: Interlayer Coupling; Spin-polarized Scanning Tunneling Microscopy.

#### Bibliography

Belashchenko K D, Tsymbal E Y, Oleinik I I, van Schilfgaarde M 2005 Positive spin polarization in Co/Al<sub>2</sub>O<sub>3</sub>/Co tunnel junctions driven by oxygen adsorption. *Phys. Rev. B* **71** (6), 224422  
 Barthélémy A, Fert A, Petroff F 1999 Giant magnetoresistance in magnetic multilayers. In: Buschow K H J (ed.) *Handbook*

*of Magnetic Materials*. Elsevier, Oxford, Vol. 12, Chap. 1, pp. 1–96  
 Bowen M, Bibes M, Barthélémy A, Contour J-P, Anane A, Lemaître Y, Fert A 2003 Nearly total spin polarization in La<sub>2/3</sub>Sr<sub>1/3</sub>MnO<sub>3</sub> from tunneling experiments. *Appl. Phys. Lett.* **82**, 233–5  
 Butler W H, Zhang X G, Schulthess T C, MacLaren J M 2001 Spin-dependent tunneling conductance of Fe|MgO/Fe sandwiches. *Phys. Rev. B* **63** (12), 054416  
 Chappert C, Fert A, Nguyen F 2007 The emergence of spin electronics in data storage. *Nat. Mater.* **6**, 813–23  
 Coehoorn R 2003 Giant magnetoresistance and magnetic interactions in exchange-biased spin valves. In: Buschow K H J (ed.) *Handbook of Magnetic Materials*. Elsevier, Amsterdam, Vol. 15, Chap. 1, pp. 1–197  
 De Groot R A, Mueller F M, Van Engen P G, Buschow K H J 1983 New class of materials: half-metallic ferromagnets. *Phys. Rev. Lett.* **50**, 2024–7  
 De Teresa J M, Barthélémy A, Fert A, Contour J P, Montaigne F, Seneor P 1999 Role of metal–oxide interface in determining the spin polarization of magnetic tunnel junctions. *Science* **286**, 507–9  
 Djayaprawira D D, Tsunekawa K, Nagai M, Maehara H, Yamagata S, Watanabe N, Yuasa S, Suzuki Y, Ando K 2005 230% room-temperature magnetoresistance in CoFeB/MgO/CoFeB magnetic tunnel junctions. *Appl. Phys. Lett.* **86** (3), 092502  
 Hertz J A, Aoi K 1973 Spin-dependent tunnelling from transition-metal ferromagnets. *Phys. Rev. B* **8**, 3252–6  
 Jullière M 1975 Tunneling between ferromagnetic films. *Phys. Lett. A* **54**, 225–6  
 Kaiser C, Panchula A F, Parkin S S P 2005a Finite tunneling spin polarization at the compensation point of rare-earth-metal–transition-metal alloys. *Phys. Rev. Lett.* **95** (4), 047202  
 Kaiser C, van Dijken S, Yang S-H, Yang H, Parkin S S P 2005b Role of tunneling matrix elements in determining the magnitude of the tunneling spin polarization of 3d transition metal ferromagnetic alloys. *Phys. Rev. Lett.* **94** (4), 247203  
 LeClair P, Kohlhepp J T, Swagten H J M, de Jonge W J M 2001 Interfacial density of states in magnetic tunnel junctions. *Phys. Rev. Lett.* **86**, 1066–9  
 LeClair P, Swagten H J M, Kohlhepp J T, van de Veerdonk R J M, de Jonge W J M 2000 Apparent spin polarization decay in Cu dusted Co/Al<sub>2</sub>O<sub>3</sub>/Co tunnel junctions. *Phys. Rev. Lett.* **84**, 2933–6  
 Lee Y M, Hayakawa J, Ikeda S, Matsukura F, Ohno H 2007 Effect of electrode composition on the tunnel magnetoresistance of pseudo-spin-valve magnetic tunnel junction with a MgO tunnel barrier. *Appl. Phys. Lett.* **90** (3), 212507  
 Mathon J, Umerski A 2001 Theory of tunneling magnetoresistance of an epitaxial Fe/MgO/Fe(001) junction. *Phys. Rev. B* **63** (4), 220403  
 Moodera J S, Kinder L R, Wong T M, Meservey R, Nowak J 1995 Large magnetoresistance at room temperature in ferromagnetic thin film tunnel junctions. *Phys. Rev. Lett.* **74**, 3273–6  
 Miyazaki T, Tezuka N 1995 Giant magnetic tunneling effect in Fe/Al<sub>2</sub>O<sub>3</sub>/Fe junction. *J. Magn. Magn. Mater.* **139**, L231–4  
 Nagahama T, Yuasa S, Tamura E, Suzuki Y 2005 Spin-dependent tunneling in magnetic tunnel junctions with a layered antiferromagnetic Cr(001) spacer: role of band structure and interface scattering. *Phys. Rev. Lett.* **95** (4), 086602  
 Oleinik I I, Tsymbal E Y, Pettifor D G 2000 Structural and electronic properties of cobalt/alumina tunnel junctions from first principles. *Phys. Rev. B* **62**, 3952–9

- Paluskar P V, Attema J J, de Wijs G A, Fiddy S, Snoeck S, Kohlhepp J T, Swagten H J M, de Groot R A, Koopmans B 2008 Spin tunneling in junctions with disordered ferromagnets. *Phys. Rev. Lett.* **100**(4), 057205
- Parkin S S P, Kaiser C, Panchula A, Rice P M, Hughes B, Samant M, Yang S-H 2004 Giant tunneling magnetoresistance at room temperature with MgO(100) tunnel barriers. *Nat. Mater.* **3**, 862–7
- Sharma M, Wang S X, Nickel H 1999 Inversion of spin polarization and tunneling magnetoresistance in spin-dependent tunneling junctions. *Phys. Rev. Lett.* **82**, 616–9
- Slonczewski J 1989 Conductance and exchange coupling of two ferromagnets separated by a tunneling barrier. *Phys. Rev. B* **39**, 6995–7002
- Stearns M B 1977 Simple explanation of tunneling spin-polarization of Fe, Co, Ni and its alloys. *J. Magn. Magn. Mater.* **5**, 167–71
- Swagten H J M 2007 Spin tunneling in magnetic junctions. In: Buschow K H J (ed.) *Handbook of Magnetic Materials*. Elsevier, Amsterdam, vol. 17, Chap. 1, pp. 1–121
- Tedrow P M, Meservey R 1971 Spin-dependent tunneling into ferromagnetic nickel. *Phys. Rev. Lett.* **26**, 192–5
- Tezuka N, Ikeda N, Sugimoto S, Inomata K 2007 Giant tunnel magnetoresistance at room temperature for junctions using full-Heusler  $\text{Co}_2\text{FeAl}_{0.5}\text{Si}_{0.5}$  electrodes. *Jpn. J. Appl. Phys.* **46**, L454–6
- Tsymbal E Y, Pettifor D G 1997 Modelling of spin-polarized electron tunnelling from 3d-ferromagnets. *J. Phys.: Condens. Matter* **9**, L411–17
- Velev J P, Belashchenko K D, Stewart D A, van Schilfgaarde M, Jaswal S S, Tsymbal E Y 2005 Negative spin polarization and large tunneling magnetoresistance in epitaxial  $\text{Co}/\text{SrTiO}_3/\text{Co}$  magnetic tunnel junctions. *Phys. Rev. Lett.* **95**(4), 216601
- Yuasa S, Nagahama T, Fukushima A, Suzuki Y, Ando K 2004 Giant room-temperature magnetoresistance in single-crystal Fe/MgO/Fe magnetic tunnel junctions. *Nat. Mater.* **3**, 868–71
- Yuasa S, Nagahama T, Suzuki Y 2002 Spin-polarized resonant tunneling in magnetic tunnel junctions. *Science* **297**, 234–7
- Yuasa S, Sato T, Tamura E, Suzuki Y, Yamamori H, Ando K, Katayama T 2000 Magnetic tunnel junctions with single-crystal electrodes: a crystal anisotropy of tunnel magnetoresistance. *Europhys. Lett.* **52**, 344–50

H. J. M. Swagten and P. V. Paluskar

Copyright © 2010 Elsevier Ltd.

All rights reserved. No part of this publication may be reproduced, stored in any retrieval system or transmitted in any form or by any means: electronic, electrostatic, magnetic tape, mechanical, photocopying, recording or otherwise, without permission in writing from the publishers.

Encyclopedia of Materials: Science and Technology  
 ISBN: 978-0-0804-3152-9  
 pp. 1–7